Volume 3, Issue 1, pp. 13-16, 2019.
International Journal of Scientific Engineering and Science
ISSN (Online): 2456-7361

Simulation of a PEM Fuel Cell Electric Vehicle

Wahib Andari, Hatem Allagui, Abdelkader Mami
UR-LAPER, Faculty of Sciences of Tunis, University of Tunis El Manar2092 Tunis, Tunisia Tunis, Tunisia

Abstract— *This paper presents the utilization of a supercapacitor (SC) as an auxiliary power source in an electric vehicle (EV), composed of a proton electrolyte membrane fuel cell (PEMFC) as the main energy source. The main weak point of PEMFC is slow dynamics because one must limit the fuel cell current slope in order to prevent fuel starvation problems, to improve its performance and lifetime. The very fast power response and high specific power of a supercapacitor can complement the slower power output of the main source to produce the compatibility and performance characteristics needed in a propulsion system. In fact, the paper reviews the model description of the vehicle with a focus on architecture and modeling of the driving chain which includes fuel cell system, a supercapacitor and the PM synchronous motor. This motor can achieve high performance than induction motor like high speed, high torque and high efficiency. A hybrid power train configuration based on a PEM fuel cell is designed and simulated by using a matlab/simulink.*

Keywords— *PEM Fuel Cell, PMSM, supercapacitor, fuel cell vehicle.*

I. INTRODUCTION

The production of electricity from renewable energy sources becomes an urgent need to get away from the dependence linked to the exploitation of fossil energy resources [1]. The fuel cell vehicles are currently considered the future's solution to reduce pollution in the transport sector. In this context the fuel cell powered in hydrogen mainly has become one of the most promising alternatives for development in several areas such as mobile phone and stationary cars [1].

The major problem posed also using this type of energy resources was, in one hand, the risk of its exhaustion, and on the other hand, its harmful effects on the environment such as the release of carbon dioxide (CO_2) and the emission of greenhouse gases that affect the global climate balance.[2]

In general, hydrogen fuel cells are environmental friendly technology that transforms incoming hydrogen into electricity and contributes to renewable energy [3], [4]. They are promising and renewable energy sources with high energy efficiency and low emissions [5]. The hydrogen fuel cells are designed to take the place of conventional internal combustion engine vehicles [6]. In addition to these advantages, there are disadvantages of having lower power density and slower power response [7]. Due to the high power density, lower operating temperatures and a low power the proton exchange membrane is the primary preference in transportation sector compared to other types of Fuel cells [8].

To overcome power delivery limitations of the PEM Fuel Cell. it is necessary to pass through by the statics converters. To solve this problem a supercapacitor that represents the secondary source is chosen to respond to power requirements of hybrid vehicle. The energy storage can be reduces the size of the fuel cell, receives the energy during braking phases and generates the power and assists the proton exchange membrane [9].

This paper is divided into five sections: The first part of the study is an introduction. The second section of this paper is a description of the PEMFC. The third section is description of the supercapacitor. The fourth section is a description of the mathematical model of PMSM In the five section we will present the simulations and the Results. The last section in this paper is a conclusion.

II. THE FUEL CELL

Hydrogen PEM fuel cells transform chemical energy to electrical and thermal energy by the simple chemical reaction. In order to get an electric current out of this reaction, hydrogen oxidation and oxygen reduction are separated by a membrane, which is conducting protons from anode to cathode side [10]. While the protons are transported through the membrane, electrons are carried by an electric circuit in which their energy can be used. Modeling of fuel cells have big interest of scientist in power electronics field, as most powerful fuel cell stacks, according to their power outputs, the uses of this sources is going more and more largest thanks to their chemical reactions technologies, to be integrated into power systems. PEM (proton exchange membrane) fuel cells are energy converters that convert chemical energy of oxygen and hydrogen into electrical energy.

The reactions for a PEM fuel cell fed with hydrogen in the anode and oxygen in the cathode are:

Anode : $H_2 \rightarrow 2H^+ + 2e^-$ (1)

Cathode : $\frac{1}{2} O_2 + 2H^+ + 2e^- \rightarrow H_2O$ (2)

Overall Reaction: $H_2 + \frac{1}{2} O_2 \rightarrow H_2O$ (3)

Figure 1 shows the different regions and the corresponding polarization effects that associated with a voltage drop in every region n .The losses originate from three sources:

- Activation Polarization
- Ohmic Polarization
- Concentration Polarization

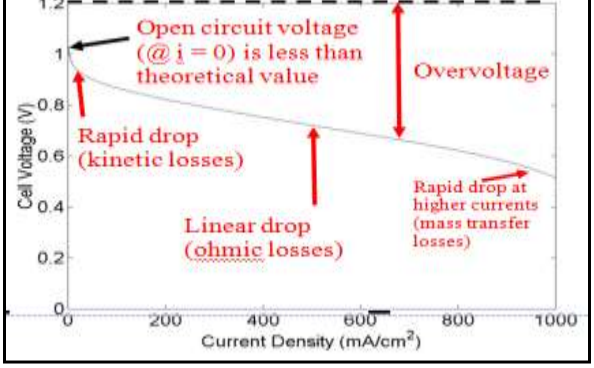

Fig. 1. Polarization plot.

A. Activation Losses

The activation over voltage is the voltage drop due to the activation of anode and cathode .It can be calculated as:

$$V_{act} = A\ln(\frac{i}{i_0}) \quad (4)$$

The constant *A* is given by equation (5):

$$A = \frac{RT}{2\alpha F} \quad (5)$$

$i_{0:\ the}$ exchange current density (A/cm^2)
T: the operating of the fuel cell [K]
α : the charge transfer coefficient. value 0 to 1.0.
F : the constant of Faraday (96.487 [C]
R: the universal gas constant 8.31451 [J]

B. Ohmic Losses

The ohmic losses are the losses in the voltage of the cell due to the resistance of electrodes to flow of electrons and the resistance of the electrolyte to the flow of ions H^+. The ohmic loss given by equation (6).

$$V_{ohmic} = iR_m \quad (6)$$

Where R_M is the equivalent resistance of the membrane (Ω).

C. Concentration Losses

The concentration losses V_{conc} are caused by the diffusion of ions through the electrolyte which produces an increase in the concentration gradient, diminishing the speed of transport and due to the mass transport. the concentration voltage can be determined by equation (7).

$$V_{conc} = -b\ln(1-\frac{j}{j_{max}})) \quad (7)$$

The constant *b* in equation 8 above is given by :

$$b = \frac{RT}{2F} \quad (8)$$

where
J: the actual current density of the cell (A/cm^2)
j_{max} : the maximum current density of fuel cell. (A/cm^2)
T: the operating of the fuel cell [K].
F : the constant of Faraday 96.487 [C].

Therefore, the output voltage of fuel cell can be expressed as:

$$V_{fc} = E_{nerst} - V_{act} - V_{ohm} - V_{conc} \quad (9)$$

Where :

$$E_{nerst} = E^0 - RT\ln\frac{PH_2\sqrt{Po_2}}{PH_2o} \quad (10)$$

E_{nerst} : the thermodynamic potential of the cell
T: the operating of the fuel cell [K].
P_{H2} , P_{O2} and P_{H2O} : the relative partial pressure of the hydrogen, oxygen and water .
R: the universal gas constant 8.31451 [J] .

The change in free Gibbs energy can be split in thermal evolution term at 1 atm and pressure variation term at temperature T and can be related to the reversible cell voltage as:

$$\Delta G = \Delta G^0 - RT\ln\frac{PH_2\sqrt{PO_2}}{PH_2O} \quad (11)$$

A 25 °C (298K), *P* = 1 atm

$$\Delta G^0 = -237.2\frac{KJ}{mol} \quad (12)$$

The change in reversible voltage at standard pressure determined by equation (13):

$$E_0 = \frac{-\Delta G^0}{nF} \quad (13)$$

Therefore, the output fuel cell voltage of a simple cell can be expressed as :

$$V_{fc} = E_{nerst} - V_{act} - V_{ohm} - V_{conc} \quad (14)$$

Where :

$$E_{nerst} = E^0 - RT\ln\frac{PH_2\sqrt{Po_2}}{PH_2o} \quad (15)$$

E_{nerst} : the thermodynamic potential of the cell
T: the operating of the fuel cell [K].
P_{H2} , P_{O2} and P_{H2O} : the relative partial pressure of the hydrogen, oxygen and water .
R: the universal gas constant 8.31451 [J] .

The change in free Gibbs energy can be split in thermal evolution term at 1 atm and pressure variation term at temperature T and can be related to the reversible cell voltage as:

$$\Delta G = \Delta G^0 - RT\ln\frac{PH_2\sqrt{PO_2}}{PH_2O} \quad (16)$$

The change in reversible voltage at standard pressure determined by equation (17):

$$E_0 = \frac{-\Delta G^0}{nF} \quad (17)$$

The parameters of the proton exchange membrane are given in table.

Parameters of PEM Fuel Cell	
Power (Kw)	1200
Current (A)	46
DC voltage (V)	26
Temperature (°C)	80
Fuel pressure (bar)	1
Air pressure(bar)	1
Length x width x height(mm)	56x25x33
Weight(Kg)	13

III. SUPERCAPACITOR

An accurate dynamic model of the SC system is essential for determining the SOC of SC [11]. Through experimental studies, it has been found that the current-to-voltage behavior of SC is significant in hybrid vehicle systems, and the net electrical dynamic behavior of SC can be predicted through approximation by an equivalent electrical circuit .In this section, the SC system model was developed based on a simple R-C_{sc} equivalent circuit model:

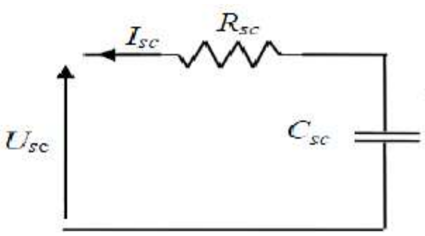

Fig. 2. Electrical model of supercapacitor (12).

The power and the output voltage of supercapacitor is defined as follow:

$$U_{sc} = V_s - R_{sc} I_{sc} \quad (18)$$

$$P_{sc} = U_{sc} . I_{sc} \quad (6)$$

Indeed, the current passing through a Supercapacitor is obtained while solving the previous equation by replacing the U_{sc} voltage by its expression:

$$R_{sc} . I_{sc}^2 - U_c . I_{sc} + P_{sc} = 0 \quad (19)$$

Hence the expression of the Supercapacitor current is defined as follows:

$$I_{sc} = \frac{U_c}{2R_{sc}} - \frac{1}{2R_{sc}} \sqrt{U_c^2 - 4R_{sc} . P_{sc}} \quad (20)$$

The state of charge SOC is expressed as follows:

$$SOC_{sc} = \frac{E_{sc}}{E_{sc_{max}}} = \frac{\frac{U_{sc}^2 * C}{2}}{\frac{U_{sc_{max}}^2 * C}{2}} = \frac{U_{sc}^2}{U_{sc_{max}}^2} \quad (21)$$

IV. THE PMSM MOTOR

Permanent magnet synchronous motors (PMSM) are widely used in low and medium power applications such as computer peripheral equipments, robotics, adjustable speed drives and electric vehicles. The growth in the market of PMSM motor drives has demanded the need of simulation tool capable of handling motor drive simulations.

Simulations have helped the process of developing new systems including motor drives, by reducing cost and time. Simulation tools have the capabilities of performing dynamic simulations of motor drives in a visual environment so as to facilitate the development of new systems.

The voltage equations of the PMSM in the rotor reference are given by

$$V_q = R_s I_q + L_q p i_q + \omega_r L_d i_d + \omega_r \varphi_f \quad (22)$$

$$V_d = R_s I_d + L_d p i_d - \omega_r L_d i_q \quad (23)$$

The mechanical torque equation is given by:

$$T_e = T_L + B\omega_m + J\frac{d\omega_m}{dt} \quad (24)$$

Where V_d and V_q are the d, q axis voltages, id , iq are the d, q axis stator currents, L_d, and L_q are the d, q axis inductances, φ_d and φ_q are the d, q axis stator flux linkages, Rs is the stator winding resistance per phase and ω_r is rotor electrical speed.

V. THE SIMULATIONS AND RESULTS

The curve shown in fig. 3 correspond to the experimental current - voltage characteristic of a commercial fuel cell model, for a gas pressure PO_2 = PH_2=2 atm and a temperature of 338 K.

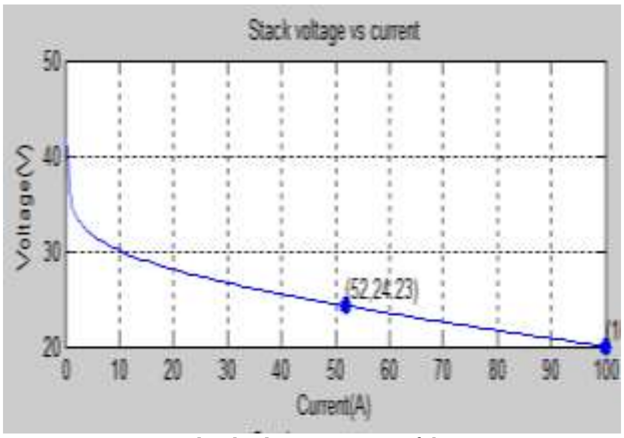

Fig. 3. Simulated polarization curve of the PEMFC.

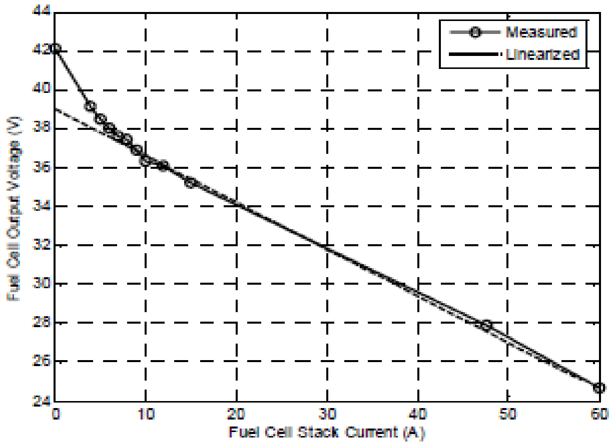

Fig. 4. Experimental polarization of the PEMFC [13].

From the curve of the characteristic voltages-currents of fig. 3, the current and the voltage are inversely proportional. Also, the voltage vacuum stack is 42 V. The voltage of stack (U_{stack} =24 V) is presented at the fuel cell when it reaches a current consumption I = 52.24 A. The activation loss, ohmic loss and concentration loss can be clearly seen in polarization curves. Fig. 4 shows the measured output characteristics of the NexaTM 1.2kW PEM fuel cell model [8]. It is observed that the simulated characteristic curve presented in fig. 3 is almost same as experimental results show in fig.4.

The fig. 5 shows the three phase currents drawn by the motor. It is clear that the current is non sinusoidal at the starting and becomes sinusoidal in the under steady state condition. Under no-load the speed value is 300 rpm.

In fig. 6, the electromagnetic torque of PMSM is larger when it started. At the beginning, system doesn't reach equilibrium because initially electromechanical time constant is much larger than electromagnetic time constant, instantaneous rate of change of stator flux linkage is larger than that of rotor flux linkage.

The simulation time is 0.04s and the speed get stable at 300rad/s at 0.027s (fig. 7) When the actual motor torque becomes less than the given value, the angle between the

International Journal of Scientific Engineering and Science
Volume 3, Issue 1, pp. 13-16, 2019. ISSN (Online): 2456-7361

stator and rotor flux linkage increases, that leads torque growing fast and vice versa, after a exact equilibrium state the torque as well as speed settles very fast to final value. At time is 0.027 the torque is constant at 3.N-m fig. 4 show the simulation output for the line Current of PMSM

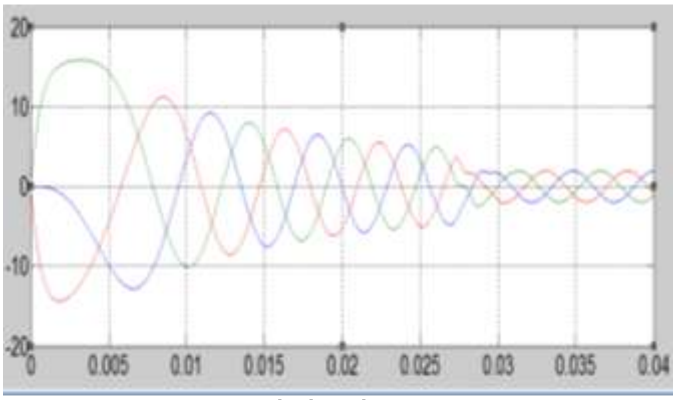

Fig. 5. The three phase current.

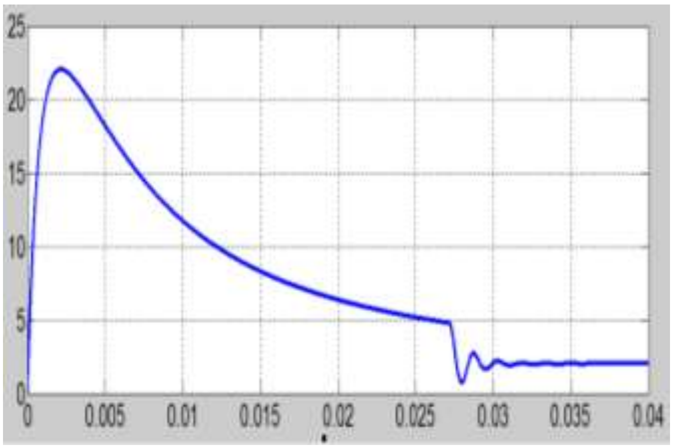

Fig. 6. The Electromagnetic torque.

Fig. 7 show the simulation output for the motor speed

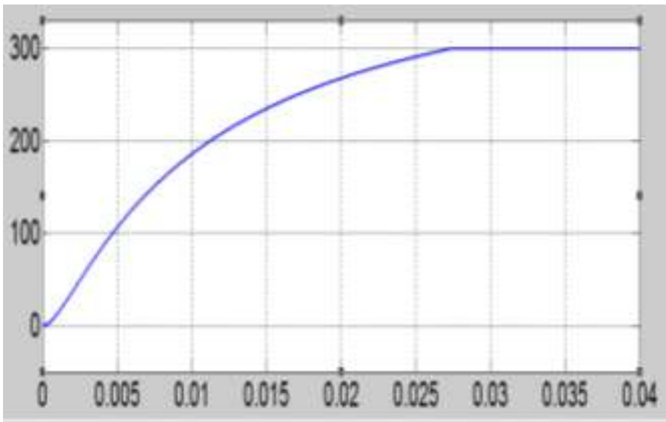

Fig. 7. The motor speed.

VI. Conclusion

In this paper, a study of hybrid PEMFC/supercapacitor bank system supplying an electric vehicle is presented.

This paper presents the case of an electrical vehicle powered by a hybrid system which consists of a fuel cell as a main source and a storage device which is supercapacitor stack as a secondary source. The obtained results show the feasibility of the hybrid system production for an electric vehicle. Simulation results under matlab-simulink wereshown to prove the validity of the presented system and their effectiveness.

References

[1] Wei Jiang, Babak Fahimi, "Active current sharing and source management in fuel cell battery hybrid power system," *IEEE Transaction on Industrial Electronics*, vol. 57, no. 2, pp. 752-761, 2010.
[2] M. U. Zunogli and M. S. Alam, "Dynamic modeling design and simulation of a PEM fuel cell/ultracapacitor hybrid system for vehicular applications", *Energy Conversion & Management*, vol. 48, no.5, pp. 1544-1553, 2007.
[3] Ke Jin, XinboRuan, Mengxiong Yang, and Min Xu, "Power management for fuel-cell power system cold start", *IEEE Transactions on Power Electronics*, vol. 24, pp. 2391-2395, 2009.
[4] J. C. Amphlett, R. M. Baumert, R. F. Mann, B. A. Peppley, and P. R. Roberge, "Performance modelling of the ballard mark iv solid polymer electrolyte fuel cell", *Journal of Electrochemical Society*, vol. 142, issue 1, pp. 9–15, 1995.
[5] Larminie J, Dicks A., *Fuel Cell Systems Explained*, 2nd ed. John Wiley & Sons Inc; 2003.
[6] J. H. Lee, T. R. Lalk, and A. J. Appleby, "Modeling electrochemical performance in large scale proton exchange membrane fuel cell stacks", *Journal of Power Sources*, vol. 70, pp. 258–268, 1998.
[7] S. R. Chaitanya, J. S. V. Sivia, and M. Rambabu, "Fuel cell supplied SVPWM controlled inverter fed PMSM drive in an electrical vehicle," *International Journal of Engineering Research & Technology Trends in Engineering*, vol. 3, 2014.
[8] Xiaoting Ye and Tao Zhang, "Direct torque control of permanent magnet synchronous motor using space vector modulation", *Proc. IEEE Chinese Control and Decision Conference*, pp. 1450-1453, 2010.
[9] Avinash Mishra, Swaraj Save, and Rohit Sen, "Space vector pulse width modulation", *International Journal of Scientific & Engineering Research*", vol. 5, issue 2, 2014.
[10] S. Nakashima, Y. Inagaki, and I. Miki, "Sensorless initialrotor position estimation of surface permanent magnet synchronous motors," *IEEE Transactions on Industry Applications*, vol. 36, issue 6, pp. 1598-1603, 2000.
[11] P. Pillay, R. Krishnan, "Modeling, simulation, and analysis of permanent-magnet motor drives, Part 1:The permanent-magnet synchronous motor drive", *IEEE Transactions on Industry Applications*, vol. 25, issue 2, pp. 265-273, 1989.
[12] P. Pillay, and R. Krishnan, "Modeling, simulation, and analysis of permanent-magnet motor drives, part I: the permanent-magnet synchronous motor drive," *IEEE Trans. Industry Applications*, vol. 25, no. 2, pp. 265-273, 1989.
[13] Shailendra Jain, Jin Jiang, Xinhong Huhang, and Srdjan Stvandic, "Single stage power electronic interface for a fuel cell based power supply system," *IEEE Electric Power Conference*, pp. 201-206, 2007.